analytical chemistry

Article

Cite This: Anal. Chem. 2019, 91, 9916−9924

pubs.acs.org/ac

Separation of Sialylated Glycan Isomers by Differential Mobility Spectrometry

Catherine S. Lane,*[,†] Kirsty McManus,[‡] Philip Widdowson,[‡] Sarah A. Flowers,[§] Gerard Powell,[‡] Ian Anderson,[‡] and J. Larry Campbell*[,∥]

[†]SCIEX, Phoenix House, Centre Park, Warrington WA1 1RX, United Kingdom

[‡]Allergan Biologics Limited, 12 Estuary Banks, Speke, Liverpool L24 8RB, United Kingdom

[§]Georgetown University, Washington, D.C., United States

[∥]SCIEX, 71 Four Valley Drive, Concord, Ontario, Canada, L4K 4 V8

ABSTRACT: Mass spectrometry has proven itself to be an important technology for characterizing intact glycoproteins, glycopeptides, and released glycans. However, these molecules often present significant challenges during analysis. For example, glycans of identical molecular weights can be present in many isomeric forms, with one form having dramatically more biological activity than the others. Discriminating among these isomeric forms using mass spectrometry alone can be daunting, which is why orthogonal techniques, such as ion mobility spectrometry, have been explored. Here, we demonstrate the use of differential mobility spectrometry (DMS) to separate isomeric glycans differing only in the linkages of sialic acid groups (e.g., α 2,3 versus α 2,6). This ability extends from a small trisaccharide species to larger biantennary systems and is driven, in part, by the role of intramolecular solvation of the charge site(s) on these ions within the DMS environment.

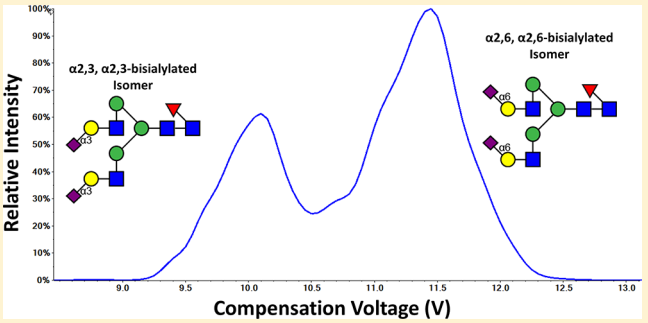

Glycosylation, a post-translational modification found on more than half of all human proteins,[1−4] can induce complex changes in both the structure and function of proteins. Glycan structures are highly variable, and even slight changes to anomeric configuration, monomer stereochemistry, or inter-residue linkage have been shown to have dramatic biological repercussions.[5−8] Therefore, there is a strong desire to gain a more complete understanding of the forms of glycosylation present on proteins, especially in the burgeoning class of monoclonal antibody-based drugs.[9] However, the high level of complexity found in protein glycosylation makes its characterization extremely challenging.

The sialic acid monosaccharide group has particularly important functions in many physiological and pathological processes, including pathogen binding and regulation of the immune response.[10] This is mediated by their almost exclusively terminal nature, typically found at the outermost ends of glycan chains. In human cells, the linkage position of a sialic acid to a glycan side chain can be α2,3 or α2,6 to a galactose residue, α2,6 to a N-acetylgalactosamine (GalNAc) residue, or α2,8 to another sialic acid residue.[11,12] The sialic acid linkage configuration has important consequences for biological function, for example, upregulation of α2,6 sialic acid via the sialyl Tn antigen is highly associated with a wide range of cancers, and a shift to expression of the α2,3 linked sialic acid can indicate metastasis in certain cancers.[13] For the development of biopharmaceuticals, characterization of sialylation is essential for determination of function and efficacy.[9]

Mass spectrometry (MS), a very useful technique for characterization of protein glycosylation,[14,15] necessarily relies on orthogonal front-end techniques for the separation of isobaric and isomeric glycosylation products. Many of these species have identical molecular weights (m/z values) and, when fragmented in an MS/MS experiment, yield almost identical fragment ion patterns. The relative intensities of these fragments can sometimes differ between isomeric glycan ions, but when analyzed as a mixture, the analytical utility of such ion ratios can be rendered futile. While a wide range of glycan and glycopeptide isomers can be separated using the traditional coupling of liquid chromatography (LC) to MS, sialylated N-glycan α2,3 and α2,6 linkage isomers present a significant LC challenge. Recent strategies to address this have used linkage-specific derivatization,[16−18] capillary electrophoresis,[19] and specialized HILIC techniques, which still maintained a derivatization element[18,20] or involved online processing[21] in their workflows.

As an alternative to chromatographic and electrophoretic technologies, ion mobility techniques are being investigated as

Received: March 30, 2019
Accepted: June 18, 2019
Published: June 18, 2019

DOI: 10.1021/acs.analchem.9b01595
Anal. Chem. 2019, 91, 9916−9924

a means of separation for isobaric glycans and glycopeptides.[22−37] However, only three studies to date have focused on the differentiation of α2,3- from α2,6-sialylation,[27,31,36] and all of these utilized traveling-wave ion mobility spectrometry (TWIMS). While small isomeric glycans exhibit drift times that allow for differentiation,[27,31] only partial separation has been afforded for larger biantennary species.[36]

In this study, we explore the potential of using differential mobility spectrometry (DMS)[38−42] (also known as high-field asymmetric waveform ion mobility (FAIMS)) to differentiate sialic acid linkage isomers. In these experiments, chemical modifiers can be added to the DMS cell to enhance the degree of separation. In DMS experiments, ions are carried between two planar, parallel electrodes to which is applied a radio frequency asymmetric voltage (separation voltage or SV). This establishes dynamic high- and low-electric field conditions,[40] and as the SV is increased, ions begin to acquire "zig-zag" trajectories of larger amplitude as they traverse the DMS cell. This off-axis component to the trajectory increases nonlinearly with increasing SV. To bring their flight paths back on axis for successful sampling by a mass spectrometer, ions require a dc compensation voltage (CV) to provide this restorative trajectory. Subsequent to DMS separation, further verification of the isomeric forms may be conducted by tandem mass spectrometry using either diagnostic fragment ions or fragmentation patterns (if the glycan structures allow). In this study, we aimed to assess the capability of DMS-MS to separate α2,3 and α2,6 sialylated glycan isomers, and to employ molecular modeling tools to present hypotheses that explain differences between the isomers in their observed DMS behaviors.

METHODS

Sample Preparation. Three α2,3 and α2,6 sialic acid-containing isomer pairs were analyzed in this study (Figure 1). Two of the pairs, depicted in Figure 1A and B, were purchased from Dextra Laboratories (Reading, UK). The larger isomer pair (Figure 1C) was purchased from TheraProteins (Barcarena, Portugal). For ease of reference, the glycan compositions of the isomer pairs are given in terms of the numbers of hexose (H), *N*-acetylhexosamine (N), fucose (F), and *N*-acetylneuraminic acid (S) units. The working ESI solutions of these glycans were prepared in acetonitrile and water (20/80, v/v) containing 10 mM ammonium bicarbonate, to concentrations of 1−25 μg/mL. Isomeric glycans were analyzed individually to assess their characteristic DMS behaviors (vide supra) and also to identify any unique MS/MS fragmentation patterns. The same isomer pairs were also analyzed as mixtures to evaluate the DMS separation of these pairings.

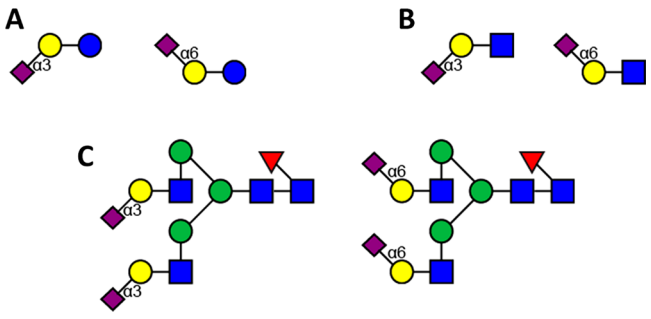

Figure 1. Glycan pairs analyzed in this study, depicted using the Symbol Nomenclature for Glycans (SNFG) format.[43,44] For ease of reference, the glycan compositions of the isomer pairs are given in terms of the numbers of hexose (H), *N*-acetylhexosamine (N), fucose (F), and *N*-acetylneuraminic acid (S) units. (A) H2S1, representing both Neu5Acα2-3Galβ1-4Glc (CAS #: 35890-38-1) and Neu5Acα2-6Galβ1-4Glc (CAS #: 35890-39-2); (B) H1N1S1, representing both Neu5Acα2-3Galβ1-4GlcNAc (CAS #: 81693-22-3) and Neu5Acα2-6Galβ1-4GlcNAc (CAS #: 174757-71-2); and (C) H5N4F1S2, representing the disialylated biantennary glycan pair (α2-3 catalogue #:GTP 2N(2,3)-2A+F; α2-6 catalogue number: GTP 2N(2,6)-2A+F) (No CAS numbers available).

DMS-MS Instrumentation. Experiments were performed using either a QTRAP® 6500 or a QTRAP® 6500+ hybrid triple quadrupole−linear ion trap mass spectrometer (qLIT) (SCIEX, Concord, ON, Canada) (Figure 2A and B). Each instrument was equipped with a SelexION® differential mobility spectrometer (DMS) device (SCIEX) (Figure 2A), the fundamental properties of which have been described elsewhere.[38,41,42] The DMS cell was mounted between the sampling orifice of the mass spectrometer and a Turbo V ion source (ESI voltage of −4200 V). The temperature of the DMS cell was maintained at 150 °C, with nitrogen curtain gas operated at 30 psi. Chemical modifier (methanol) was added into the curtain gas flow at 1.5% or 3.0% (mole ratio). The DMS cell also featured a jet injector modification[45] designed to improve transmission of ions by mitigating the effects of RF fringing fields and diffusional losses at the entrance of the DMS cell.

For DMS infusion experiments, SV was stepped from 0 to 4500 V in increments of 200 to 1000 V. At each value of SV, CV was scanned from −10 V to +30 V in 0.2-V steps. At each value of CV, either multiple reaction monitoring (MRM) data (Table 1; H2S1, H1N1S1) or full scan enhanced product ion (EPI) MS/MS (H5N4F1S2) data were acquired for the glycan isomers. The resulting plots reveal the optimal CV at which the ion is transmitted through the DMS cell at a particular value of SV. If optimal CV is plotted against SV to create a "dispersion plot",[46] the curvature of the SV/CV plot can describe the behavior exhibited by the ion within the DMS cell.[39,47,48]

To enhance the DMS separation of the isomeric pairs of glycans, we employed resolving (throttle) gas[41]—added at the terminus of the DMS cell (Figure 2A)—that serves to increase the residence times for the ions within the DMS cell. This leads to narrower CV profiles for ions and higher resolution for the DMS measurements. After determination of optimal CV values for DMS-separated glycan isomers, CV values can be fixed to allow the acquisition of full scan MS/MS data for each isomer.

Linear ion trap MS/MS spectra (enhanced product ion, or EPI, scans) of individual glycan isomers were collected using the Q3 of the mass spectrometer (Figure 2B) and yielded specific ions that were either diagnostic for, or more abundant in, the α2,6 glycan isomer. For H2S1 and H1N1S1, these ions were utilized for the design of isomer-specific MRM transitions. For H5N4F1S2, the presence (or absence) of these ions in the linear ion trap MS/MS spectra of separated glycan pairs was used to confirm that the α2,3 had indeed been isolated from the α2,6 form.

All data were processed using an in-house, research-grade version of PeakView® software (SCIEX).

Computational Chemistry. The energy-optimized structures and ion/molecule binding energies were obtained by first constructing the glycan structures using a GLYCAM-Web

DOI: 10.1021/acs.analchem.9b01595
Anal. Chem. 2019, 91, 9916−9924

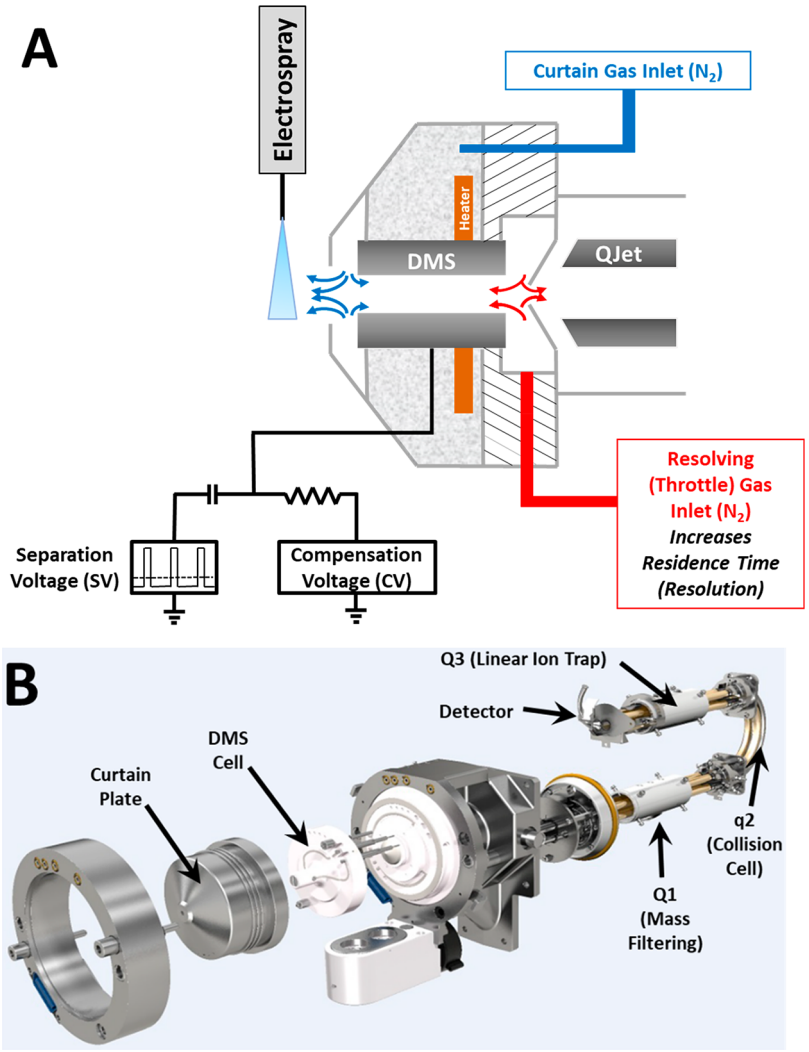

Figure 2. Schematic diagram of (A) the DMS cell coupled to (B) a hybrid triple quadrupole-linear ion trap MS system employed in this study.

Table 1. MRM Transitions and Parameter Settings for the Sialylated Trisaccharides Analyzed in This Study

Analyte	Q1m/z	Q3m/z	Collision Energy (CE, lab frame, eV)
H2S1	632.2	290.1	39
	632.2	470.2	43
	632.2	572.3	41
H1N1S1	673.2	290.1	41
	673.2	572.3	41

Carbohydrate builder (www.glycam.org),[49] which employed an AMBER MM force field optimization. An additional geometry optimization using these AMBER-optimized structures as starting points was performed using the PM7 method[50] as implemented in Gaussian 16.[51] We selected the PM7 method given its ability to calculate intra- and intermolecular hydrogen bond energies with reasonable accuracy despite their lower computational costs compared to density functional theory.[50] To determine an estimate for the anion/methanol binding energy for each glycan, we calculated the optimized geometries and energies for each unsolvated anion (without any methanol molecules present), for each anion solvated with methanol (one methanol molecule per charge site), and a lone methanol molecule in isolation. An estimate of each glycan's ion/methanol binding energy was calculated by subtracting the energies of the unsolvated anion and the isolated methanol molecule(s) from the energy of the solvated anion. A comparison of relative anion−methanol binding energies allows us to compare the impact of solvation on these species and any correlations of this property on the DMS separations observed. Structures were visualized using GaussView 16.[52]

RESULTS AND DISCUSSION

DMS Separates Sialic Acid Linkage Isomers—Trisaccharides H2S1 and H1N1S1. Given the successes of earlier ion mobility-based studies that showed some separation of α2,3 and α2,6 Neu5Ac linked glycan isomers,[27,31,36] we initiated this DMS-based study to explore its capability to perform the same separations. As mentioned previously, DMS has been used to distinguish isomeric ions,[47,48,53−61] including glycans[24] and glycopeptides.[26] For the analysis of the trisaccharide isomers (as well as the other sialylated glycans in this study), we operated the DMS-MS system in negative mode assuming the carboxylic acid groups of the sialic acid moieties would deprotonate easily. Also, having some foreknowledge about the sites of deprotonation (i.e., charging) of these ions aids in our computational analyses of these DMS experiments. For example, it has been shown that ions' sites of charging are the focal points of the ion/molecule clustering

DOI: 10.1021/acs.analchem.9b01595
Anal. Chem. 2019, 91, 9916−9924

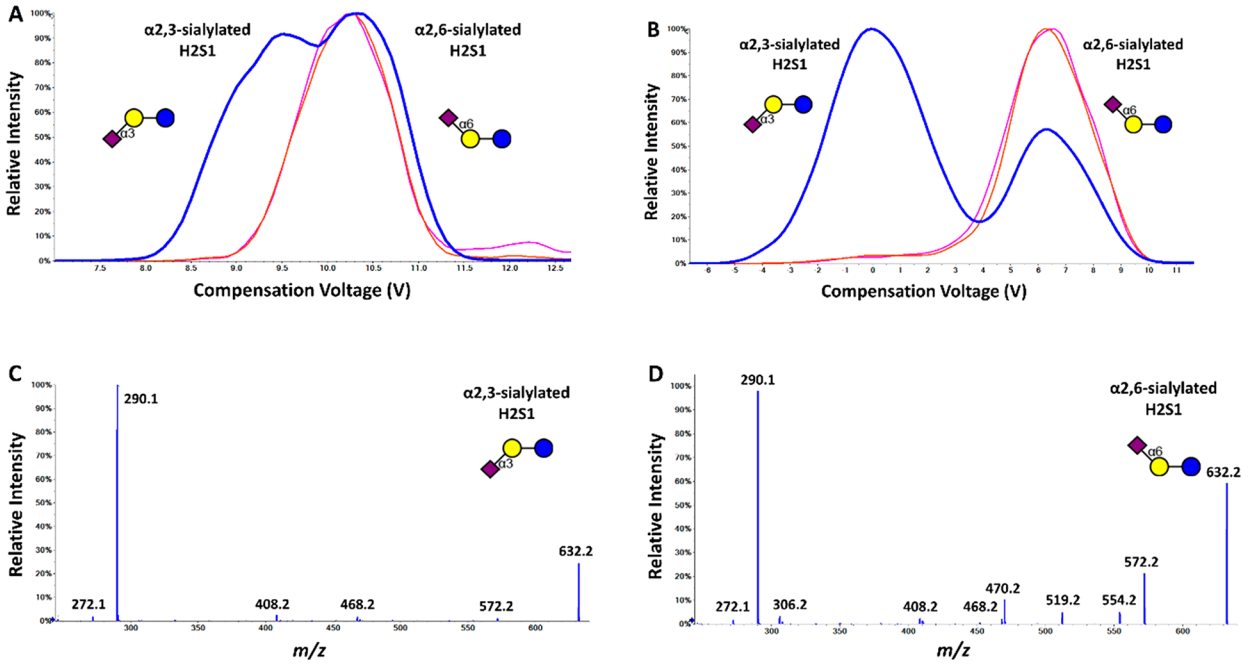

Figure 3. Separation of deprotonated sialylated glycans H2S1 using DMS. The blue trace was obtained during the analysis of the mixture of the two isomers, while the red and pink traces were produced during the analysis of only the H2S1 isomer. While minimal separation is observed when the DMS is operated at SV = 4500 V using nitrogen alone as the carrier gas (A), the α2,3 and α2,6 sialic acid-linked isomers were fully separated when methanol was added to the carrier gas. Full scan MS/MS spectra (collision energy = 45 eV, lab frame for both spectra) obtained using the SV and CoV settings for full separation, show different fragment patterns for the α2,3 (C) and the α2,6 isomers (D). Note, the presence of a α2,6 isomer-specific ^{0,4}A2-CO_2 fragment at *m/z* 306 (D).

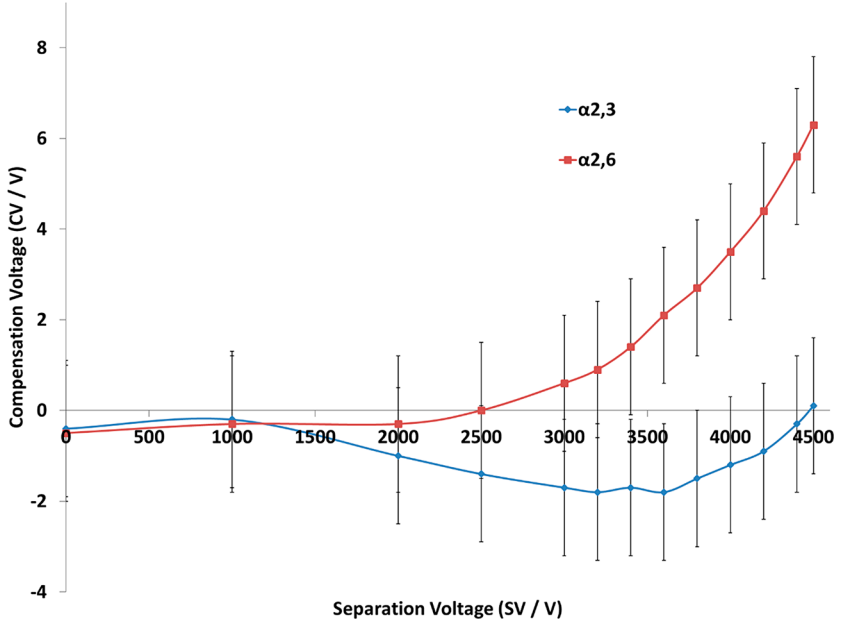

Figure 4. Dispersion plots (CV versus SV response) for two H2S1 isomers analyzed with the DMS cell's carrier gas doped with 1.5% methanol. The more negative CV for the α2,3 isomer reveals a stronger binding interaction between these ions and methanol than for the α2,6 isomers. Error bars represent the full width at half-maximum for each CV measurement (~3.0 V).

events so critical to establishing unique DMS behavior for ions, allowing for their separation in compensation voltage (CV).[47,62]

Initially, we infused a mixture of the two isomeric H2S1 trisaccharides (Figure 1a) into the ESI source, generating deprotonated forms of both isomer. These isomeric ions were then sampled by the DMS using only nitrogen as the carrier gas. With the SV set to 4500 V and resolving gas set at high, we observed marginal separation of the two isomers in CV space (Figure 3A) as the CV was ramped (*x*-axis of Figure 3A). The blue trace marks the response for the MRM transition of 632.2/290.1 (common to both isomers). However, the pink and red MRM traces (632.2/470.2 and 632.2/572.3) are predominantly observed for the α2,6 isomer (verified by independent analysis of that isomer). These traces reveal that the α2,6 isomer is transmitted at the more positive CV (~10.3

DOI: 10.1021/acs.analchem.9b01595
Anal. Chem. 2019, 91, 9916−9924

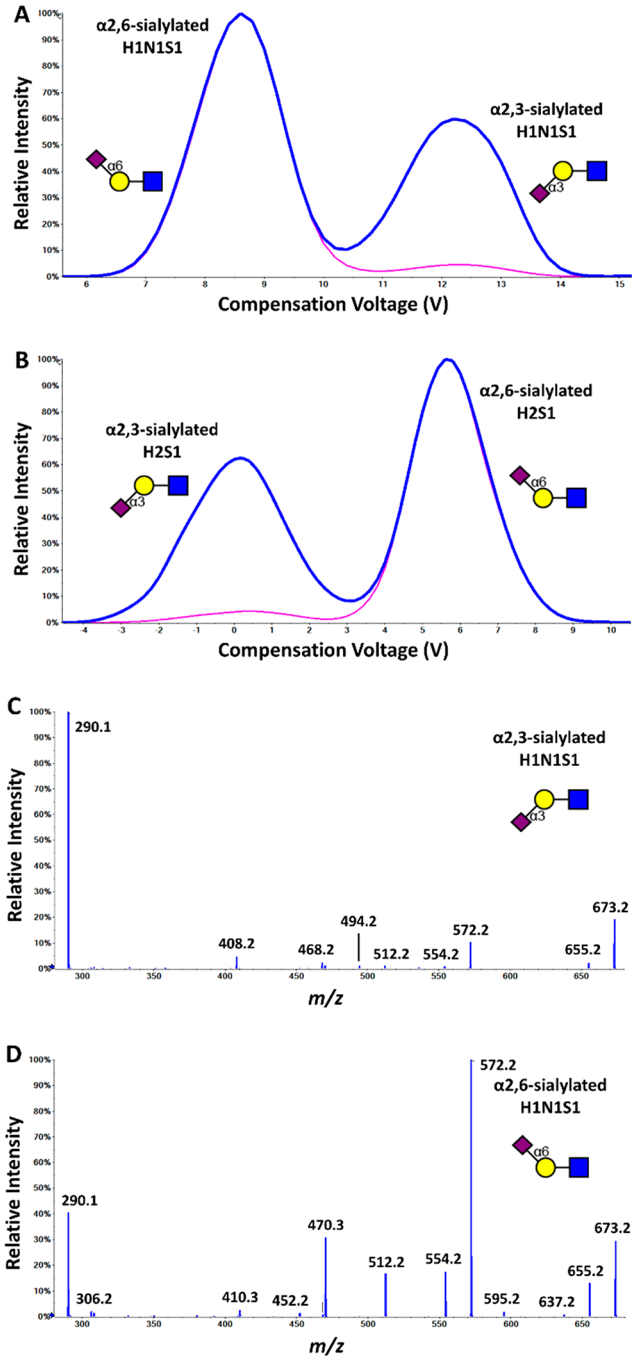

Figure 5. Separation of the deprotonated sialylated glycans H1N1S1 using DMS. The α2,3 and α2,6-sialylated isomers were fully separated when pure nitrogen (A) or methanol-doped nitrogen (B) was used as the carrier gas. However, a higher setting of resolution gas was needed to separate the isomers in the absence of methanol (resolution gas set to medium (A), or low (B)) Full scan MS/MS, obtained using the SV and CoV settings for full separation, shows different fragment patterns for the α2,3 (C) and the α2,6 isomers (D). Note, the presence of a α2,6 isomer-specific $^{0,4}A_2$-CO_2 fragment at m/z 306 (D).

V) than the α2,3 variant (~9.4 V). The H2S1 α2,3 and α2,6 isomers produce different relative amounts of two large sialic acid containing fragments (Figure 3C and 3D): the m/z 572.18 cross-ring Glc fragment and m/z 470.15 c fragment are of much greater abundance in the α2,6 isomer. Although these fragments are not specific to the α2,6 isomer, the α2,6 linked sialic acid is less labile than the α2,3 linked sialic acid, making it more likely that larger fragments containing sialic acid are produced.[63]

Since these initial DMS conditions did not separate the glycan isomers, we altered the chemical environment of the DMS cell by adding volatile polar molecules to the carrier gas. This serves to probe any subtle differences in how the isomeric ions might differently cluster with these volatile molecules. Different interactions for the isomers can yield different optimal CVs that provide better separation than nitrogen alone. In this case for the H2S1 sialic acid isomers, we introduced methanol vapor into the DMS cell, and this induced different optimal CV shifts and baseline separation of the α2,3 and α2,6 isomers (Figure 3B). Another important consequence of the use of chemical modifiers is that isomer separation for these smaller glycans in the presence of methanol requires lower settings of resolution gas, which itself can drop the ion signal during its use.[41]

Besides observing MRM transitions for these H2S1 isomers, we also collected full-scan MS/MS spectra (collected at the same collision energy (lab frame) of 45 eV) for the DMS-separated α2,3 and α2,6 isomers (Figure 3C and D). Here, we observed differences in the fragmentation patterns of the two isomers (e.g., the α2,6 isomer-specific $^{0,4}A_2$-CO_2 fragment at m/z 306)[64] that provided further confirmation on the isomer separation provided by the DMS technology.

Structural Significance of the Compensation Voltage Ordering of the Glycan Isomers. Based upon the findings of previous studies,[47,48,54] the more negative CV shift exhibited for the α2,3 isomer of the H2S1 pair suggests that the ion/molecule binding energy between this anion and methanol is stronger than for the α2,6 isomer. We probed this theory further by calculating the relative binding energies of each glycan isomer with methanol, and indeed, we calculated a stronger binding energy for the α2,3 isomer (vide infra). In addition, the baseline separation displayed in Figure 3B was obtained at a SV setting of 4500 V, which was employed to highlight the maximum separation power of this DMS system. A lower SV setting (e.g., 4000 V or less) should also be sufficient to provide adequate analytical separation of these two species and would yield a slightly more intense signal for these molecules. Again, the separation of the isomers was confirmed by the presence of the α2,6-specific species at the more positive CV. These findings are depicted in the dispersion plots of Figure 4, which display the separation of the isomers' signals in SV and CV space as well as the different minimum CVs acquired by each isomer. Again, one can observe that optimal CVs for the α2,3 isomer are much more negative than the α2,6 isomer at SV values greater than 2500 V.

We next ionized a mixture of the two isomeric H1N1S1 trisaccharides (Figure 1b) to evaluate the ability of DMS to separate these species. Figure 5A displays the separation in CV space that the DMS provided using only nitrogen as the carrier gas. Here, in contrast to the H2S1 results, we observed separation of the two isomers, again verified by the presence of α2,6-isomer specific MS/MS fragments[64] being transmitted at a unique CV (+8.6 V in this case). Interestingly, while this glycan pair differs from the H2S1 isomer pair only by the added N-acetyl group on the Glc moiety, there was a notable "reversal" in the order of transmission of the isomers in the DMS (i.e., the α2,6 isomer was transmitted at a more negative CV than the α2,3 isomer). The reason for this switch is presently under investigation. Figure 5A displays the MRM

DOI: 10.1021/acs.analchem.9b01595
Anal. Chem. 2019, 91, 9916−9924

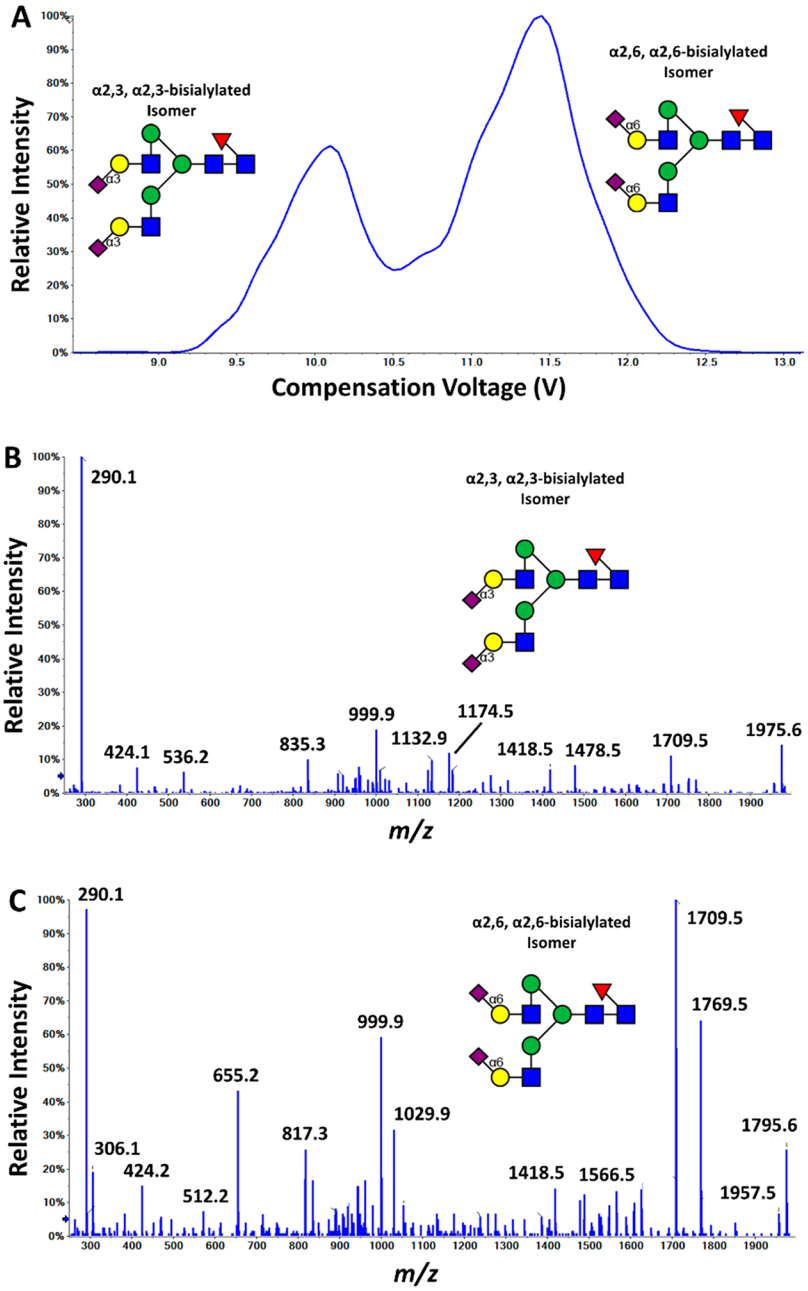

Figure 6. Separation of a pair of doubly deprotonated complex fucosylated disialylated biantennary glycans, H5N4F1S2 (A) using DMS with methanol in the carrier gas; the signal monitored is the total ion current resulting from the full-scan MS/MS analysis of both isomers as a function of CV. These full scan MS/MS spectra (B, C), obtained at CV = +10 V and CV = +11.5 V (respectively) show different fragmentation patterns, including α2,6-isomer-specific fragment ions at m/z 306 ($^{0,4}A_2$-CO_2 ion) and 655 (B_3 ion) in the spectrum C.

traces detected for these isomers: the blue trace marks the response for the MRM transition of 673.2/290.1 (common to both isomers) while the pink MRM trace (673.2/572.3) is provided predominantly by the α2,6 isomer (again, this was verified by independent analysis of that isomer).

However, just like the H2S1 analogues (Figure 3), when we added methanol to the carrier gas of the DMS cell, the α2,3 isomer of the H1N1S1 pair was transmitted at a more negative CV than the α2,6 isomer (Figure 5B, same MRM traces as A). This was consistent with the H2S1 isomer behavior and, again, suggests stronger ion/molecule binding between the methanol molecules and the α2,3 structure, which was verified by calculated binding energies (vide infra). Like the H2S1 analyses, full-scan MS/MS fragmentation patterns collected at the same collision energy (45 eV, lab frame) verified the separation and identification of the individual isomers.[64]

DMS Separates Larger Sialic Acid Linkage Isomers—Fucosylated Disialylated Biantennary Glycans H5N4F1S2. Following the successful separations of these two smaller glycan isomer pairs differing only in their sialic acid linkages, the DMS behavior of a pair of doubly deprotonated complex fucosylated disialylated biantennary glycans (H5N4F1S2) was examined. When these species were subjected to ESI in negative ion mode, they each produced abundant signals corresponding to the doubly deprotonated ($[M - 2H]^{2-}$) forms of these molecules.[63] Under nitrogen-only conditions within the DMS cell, these two isomeric ions, both present at m/z 1183.3, were inseparable (data not

DOI: 10.1021/acs.analchem.9b01595
Anal. Chem. 2019, 91, 9916−9924

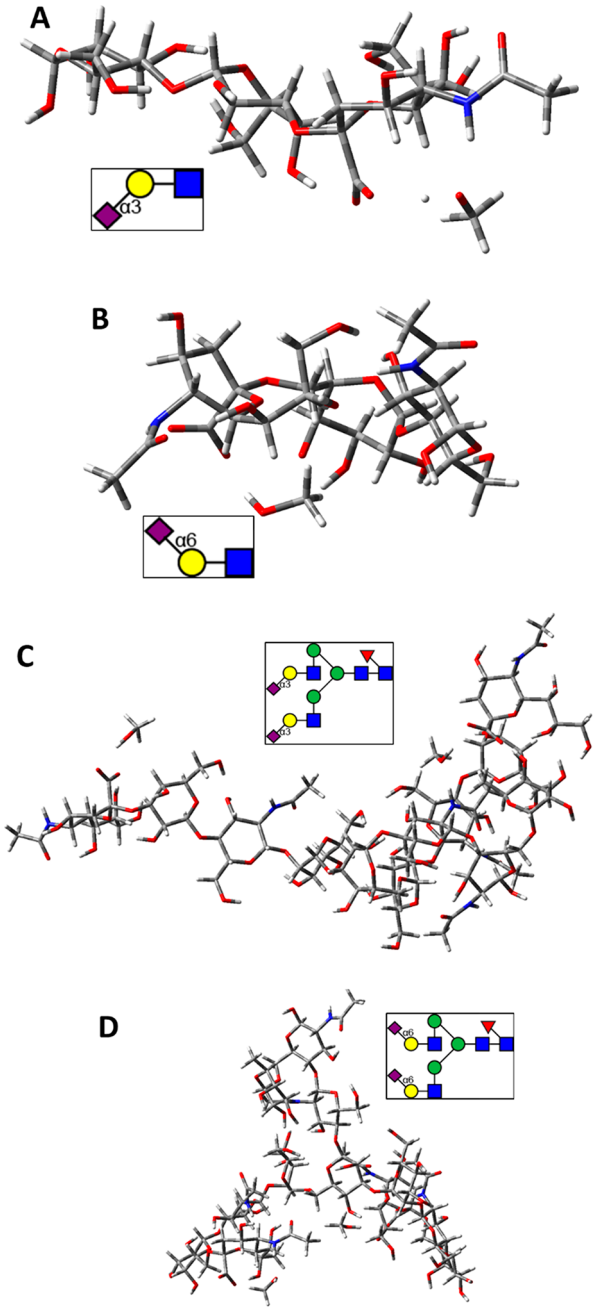

Figure 7. PM7-optimized structures of the anion−methanol complex of (A) the α2,3 and (B) the α2,6 sialic acid isomers of H1S1N1. PM7-optimized structures of the anion−methanol complex of the doubly α2,3 and doubly α2,6 sialylated isomers of H5N4F1S2 are depicted in (C) and (D). Insets depict the glycan structures in SFNG format.

shown). This led to the use of methanol to try to separate these isomers in terms of CV by exploiting any difference in the binding energies each ion exhibits with methanol molecules. These DMS conditions did provide separation for this large glycan pair, again providing a more negative CV for the doubly α2,3 sialylated isomer than for its doubly α2,6 sialylated analogue (Figure 6A). This separation also required the use of high SV (4000 V or greater), as well as the use of resolving gas (30 psi), which increases ion residence time (and resolution of DMS measurements).[41] In addition, corresponding CID MS/MS data (collision energy = 60 eV, lab frame) allowed differentiation of the α2,3 from the α2,6 isomer based on diagnostic fragment ions (Figure 6B and C).[64]

The more challenging conditions required for the DMS separation of the H5N4F1S2 isomers is echoed in another example in the literature of ion mobility separation of similar glycan isomers. Using TWIMS, Barroso and co-workers[36] also performed extensive parameter optimization to yield only partial separation of nonfucosylated H5N4S2 isomers; the addition of a fucose unit to these species resulted in their complete convolution. In our study, we were able to obtain separation of these differentially sialylated glycans by exploiting the differences in how each of these species bind to methanol molecules in the gas phase. While these differences in DMS behavior could be indicative of relative differences between the physicochemical properties of these isomers,[48,54] further studies into these and several other glycan isomers must be conducted.

Computational Chemistry Reveals Details about the DMS Separation of the Sialic Acid Linkage Isomers. The calculated methanol/glycan binding energies for each isomer supported the difference in CV shifts experienced by each ion. As expected, the isomer that is more strongly bound to two molecules of methanol (one each at the sialic acid sites) was the doubly α2,3 sialylated isomer by −6.25 kcal/mol. The structures are depicted in Figure 7C and 7D. This calculated outcome mirrored that for the smaller H1N1S1 isomers, with the α2,3 isomer binding −3.6 kcal/mol more strongly to methanol than the α2,6 analogue (structures depicted in Figure 7A and B), with the α2,3 isomer also exhibiting a more negative CV than the α2,6 pair.[48,54] The same finding was determined upon calculations of the ion/methanol binding energies for the H2S1 isomer pairs, with the α2,3 isomer binding a molecule of methanol some −10.4 kcal/mol more strongly that the α2,6 isomer. While these trends support previous DMS studies that relate ion/molecule binding energies to relative CV shifts for isomeric sets,[48,54,65] more comprehensive and higher-level computational evaluations of these structures are presently underway to provide the most accurate assessment of this property.

CONCLUSIONS

In this study, differential mobility spectrometry (DMS) was used to analyze pairs of mono- and disialylated glycan isomers. With the addition of methanol chemical modifier to the DMS, the α2,3 sialylated isomer was successfully separated from the α2,6 form (including separation of a doubly α2,3 silaylated isomer from its doubly α2,6 sialylated form) in all three isomer pairs studied, despite the varying sizes of the glycans. In addition, a more negative CV value was consistently observed for the α2,3 form than for the α2,6 form, which correlates with the stronger methanol binding energies calculated for the α2,3 isomers versus their α2,6 forms. The use of DMS to distinguish differentially sialylated glycan forms was effective with all species studied, and the trends observed show considerable promise for a wider range of sialylated glycan isomers.

AUTHOR INFORMATION

Corresponding Authors

*E-mail: cathy.lane@sciex.com.
*E-mail: larry.campbell@sciex.com.

ORCID

Sarah A. Flowers: 0000-0002-3513-2260

DOI: 10.1021/acs.analchem.9b01595
Anal. Chem. 2019, 91, 9916−9924

J. Larry Campbell: 0000-0002-4496-7171

Notes

The authors declare the following competing financial interest(s): Catherine S. Lane and J. Larry Campbell are employed by AB SCIEX, which sells the differential mobility spectrometry technology employed in the studies outlined in this manuscript.

■ ACKNOWLEDGMENTS

The authors would like to thank Christie Hunter, Yves Le Blanc, and Brad Schneider (SCIEX) and Scott Hopkins (University of Waterloo) for constructive feedback and discussions. S.A.F. would like to thank the National Institutes of Health (R56AG062305) for support.

■ REFERENCES

(1) Apweiler, R.; Hermjakob, H.; Sharon, N. *Biochim. Biophys. Acta, Gen. Subj.* **1999**, *1473*, 4−8.
(2) Corfield, A. P.; Berry, M. *Trends Biochem. Sci.* **2015**, *40*, 351−359.
(3) Abou-Abbass, H.; Abou-El-Hassan, H.; Bahmad, H.; Zibara, K.; Zebian, A.; Youssef, R.; Ismail, J.; Zhu, R.; Zhou, S.; Dong, X.; Nasser, M.; Bahmad, M.; Darwish, H.; Mechref, Y.; Kobeissy, F. *Electrophoresis* **2016**, *37*, 1549−1561.
(4) Zhu, F.; Trinidad, J. C.; Clemmer, D. E. *J. Am. Soc. Mass Spectrom.* **2015**, *26*, 1092−1102.
(5) Suzuki, Y.; Ito, T.; Suzuki, T.; Holland, R. E., Jr.; Chambers, T. M.; Kiso, M.; Ishida, H.; Kawaoka, Y. *Journal of virology.* **2000**, *74*, 11825−31.
(6) Nagae, M.; Yamaguchy, Y. *International journal of molecular sciences.* **2012**, *13*, 8398−8429.
(7) Flowers, S. A.; Ali, L.; Lane, C. S.; Olin, M.; Karlsson, N. G. *Mol. Cell. Proteomics* **2013**, *12*, 921−931.
(8) Reusch, D.; Tejada, M. L. *Glycobiology* **2015**, *25*, 1325−1334.
(9) Jefferis, R. *Nat. Rev. Drug Discovery* **2009**, *8*, 226−234.
(10) Varki, A. *Trends Mol. Med.* **2008**, *14*, 351−360.
(11) Tsuji, S. *J. Biochem.* **1996**, *120*, 1−13.
(12) Wang, P. *J. Cancer Mol.* **2005**, *1*, 73−81.
(13) Pearce, O. M.; Laubli, H. *Glycobiology* **2016**, *26*, 111−128.
(14) Rudd, P.; Karlsson, N. G.; Khoo, K.-H.; Packer, N. H. Glycomics and glycoproteomics. In *Essentials of Glycobiology*; Varki, A., Cummings, R. D., Esko, J. D., Stanley, P., Hart, G. W., Aebi, M., Darvill, A. G., Kinoshita, T., Packer, N. H., Prestegard, J. H., Schnaar, R. L., Seeberger, P. H., Eds.; Cold Spring Harbor Laboratory Press: New York, 2015-2017; https://www.ncbi.nlm.nih.gov/books/NBK453015/.
(15) Leymarie, N.; Zaia, J. *Anal. Chem.* **2012**, *84*, 3040−3048.
(16) Giménez, E.; Balmaña, M.; Figueras, J.; Fort, E.; Bolós, C.; Sanz-Nebot, V.; Peracaula, R.; Rizzi, A. *Anal. Chim. Acta* **2015**, *866*, 59−68.
(17) Parker, R. B.; McCombs, J. E.; Kohler, J. J. *ACS Chem. Biol.* **2012**, *7*, 1509−1514.
(18) Tousi, F.; Bones, J.; Hancock, W. S.; Hincapie, M. *Anal. Chem.* **2013**, *85*, 8421−8428.
(19) Kammeijer, G. S. M.; Jansen, B. C.; Kohler, I.; Heemskerk, A. A. M.; Mayboroda, O. A.; Hensbergen, P. J.; Schappler, J.; Wuhrer, M. *Sci. Rep.* **2017**, *7*, 3733.
(20) Tao, S.; Huang, Y.; Boyes, B. E.; Orlando, R. *Anal. Chem.* **2014**, *86*, 10584−10590.
(21) Yan, J.; Ding, J.; Jin, G.; Yu, D.; Yu, L.; Long, Z.; Guo, Z.; Chai, W.; Liang, X. *Anal. Chem.* **2018**, *90*, 3174−3182.
(22) Harvey, D. J.; Scarff, C. A.; Edgeworth, M.; Struwe, W. B.; Pagel, K.; Thalassinos, K.; Crispin, M.; Scrivens, J. *J. Mass Spectrom.* **2016**, *51*, 219−235.
(23) Harvey, D. J.; Scarff, C. A.; Edgeworth, M.; Pagel, K.; Thalassinos, K.; Struwe, W. B.; Crispin, M.; Scrivens, J. H. *J. Mass Spectrom.* **2016**, *51*, 1064−1079.
(24) Gabryelski, W.; Froese, K. L. *J. Am. Soc. Mass Spectrom.* **2003**, *14*, 265−277.
(25) Creese, A. J.; Cooper, H. J. *Anal. Chem.* **2012**, *84*, 2597−2601.
(26) Campbell, J. L.; Baba, T.; Liu, C.; Lane, C. S.; Le Blanc, J. C. Y.; Hager, J. W. *J. Am. Soc. Mass Spectrom.* **2017**, *28*, 1374−1381.
(27) Hinneburg, H.; Hofmann, J.; Struwe, W. B.; Thader, A.; Altmann, F.; Varón Silva, D.; Seeberger, P. H.; Pagel, K.; Kolarich, D. *Chem. Commun.* **2016**, *52*, 4381−4384.
(28) Harvey, D. J.; Scarff, C. A.; Edgeworth, M.; Crispin, M.; Scanlan, C. N.; Sobott, F.; Allman, S.; Baruah, K.; Pritchard, L.; Scrivens, J. H. *Electrophoresis* **2013**, *34*, 2368−2378.
(29) Zheng, X.; Zhang, X.; Schocker, N. S.; Renslow, R. S.; Orton, D. J.; Khamsi, J.; Ashmus, R. A.; Almeida, I. C.; Tang, K.; Costello, C. E.; Smith, R. D.; Michael, K.; Baker, E. S. *Anal. Bioanal. Chem.* **2017**, *409*, 467−476.
(30) Pu, Y.; Ridgeway, M. E.; Glaskin, R. S.; Park, M. A.; Costello, C. E.; Lin, C. *Anal. Chem.* **2016**, *88*, 3440−3443.
(31) Guttman, M.; Lee, K. K. *Anal. Chem.* **2016**, *88*, 5212−5217.
(32) Hofmann, J.; Stuckmann, A.; Crispin, M.; Harvey, D. J.; Pagel, K.; Struwe, W. B. *Anal. Chem.* **2017**, *89*, 2318−2325.
(33) Hofmann, J.; Hahm, H. S.; Seeberger, P. H.; Pagel, K. *Nature* **2015**, *526*, 241−244.
(34) Hernandez, O.; Isenberg, S.; Steinmetz, V.; Glish, G. L.; Maître, P. *J. Phys. Chem. A* **2015**, *119*, 6057−6064.
(35) Seo, Y.; Andaya, A.; Leary, J. A. *Anal. Chem.* **2012**, *84*, 2416−2423.
(36) Barroso, A.; Giménez, E.; Konijnenberg, A.; Sancho, J.; Sanz-Nebot, V.; Sobott, F. *J. Proteomics* **2018**, *173*, 22−31.
(37) Bitto, D.; Harvey, D. J.; Halldorsson, S.; Doores, K. J.; Pritchard, L. K.; Huiskonen, J. T.; Bowden, T. A.; Crispin, M. Determination of N-linked glycosylation in viral glycoproteins by negative ion mass spectrometry and ion mobility. In *Carbohydrate-based Vaccines: Methods and Protocols*; Lepenies, B., Ed.; Springer: New York, 2015; pp 93−121.
(38) Shvartsburg, A. A. *Differential ion mobility spectrometry: nonlinear ion transport and fundamentals of FAIMS*; CRC Press: Boca Raton, 2009.
(39) Purves, R. W.; Guevremont, R. *Anal. Chem.* **1999**, *71*, 2346−2357.
(40) Harvey, D. J.; Scarff, C. A.; Edgeworth, M.; Pagel, K.; Thalassinos, K.; Struwe, W. B.; Crispin, M.; Scrivens, J. H. *J. Mass Spectrom.* **2016**, *51*, 1064−1079.
(41) Schneider, B. B.; Covey, T. R.; Coy, S. L.; Krylov, E. V.; Nazarov, E. G. *Int. J. Mass Spectrom.* **2010**, *298*, 45−54.
(42) Schneider, B. B.; Nazarov, E. G.; Londry, F.; Vouros, P.; Covey, T. R. *Mass Spectrom. Rev.* **2016**, *35*, 687−737.
(43) Varki, A.; Sharon, N. In *Essentials of Glycobiology*, 2nd ed.; Varki, A., Cummings, R. D., Esko, J. D., Freeze, H. H., Stanley, P., Bertozzi, C. R., Hart, G. W., Etzler, M. E., Eds.; Cold Spring Harbor: New York, 2009.
(44) Varki, A.; Cummings, R. D.; Aebi, M.; Packer, N. H.; Seeberger, P. H.; Esko, J. D.; Stanley, P.; Hart, G.; Darvill, A.; Kinoshita, T.; Prestegard, J. J.; Schnaar, R. L.; Freeze, H. H.; Marth, J. D.; Bertozzi, C. R.; Etzler, M. E.; Frank, M.; Vliegenthart, J. F.; Lutteke, T.; Perez, S.; Bolton, E.; Rudd, P.; Paulson, J.; Kanehisa, M.; Toukach, P.; Aoki-Kinoshita, K. F.; Dell, A.; Narimatsu, H.; York, W.; Taniguchi, N.; Kornfeld, S. *Glycobiology* **2015**, *25*, 1323−1324.
(45) Schneider, B. B.; Londry, F.; Nazarov, E. G.; Kang, Y.; Covey, T. R. *J. Am. Soc. Mass Spectrom.* **2017**, *28*, 2151−2159.
(46) Levin, D. S.; Miller, R. A.; Nazarov, E. G.; Vouros, P. *Anal. Chem.* **2006**, *78*, 5443−5452.
(47) Campbell, J. L.; Zhu, M.; Hopkins, W. S. *J. Am. Soc. Mass Spectrom.* **2014**, *25*, 1583−1591.
(48) Liu, C.; Le Blanc, J. C. Y.; Schneider, B. B.; Shields, J.; Federico, J. J., III; Zhang, H.; Stroh, J. G.; Kauffman, G. W.; Kung, D. W.; Ieritano, C.; Shepherson, E.; Verbuyst, M.; Melo, L.; Hasan, M.; Naser, D.; Janiszewski, J. S.; Hopkins, W. S.; Campbell, J. L. *ACS Cent. Sci.* **2017**, *3*, 101−109.

DOI: 10.1021/acs.analchem.9b01595
Anal. Chem. 2019, 91, 9916−9924

(49) Woods Group. *GLYCAM Web*; Complex Carbohydrate Research Center, University of Georgia: Athens, GA, 2005−2018 (http://glycam.org), Access date: 06 February 2018.
(50) Frisch, M. J.; Trucks, G. W.; Schlegel, H. B.; Scuseria, G. E.; Robb, M. A.; Cheeseman, J. R.; Scalmani, G.; Barone, V.; Petersson, G. A.; Nakatsuji, H.; Li, X.; Caricato, M.; Marenich, A. V.; Bloino, J.; Janesko, B. G.; Gomperts, R.; Mennucci, B.; Hratchian, H. P.; Ortiz, J. V.; Izmaylov, A. F.; Sonnenberg, J. L.; Williams-Young, D.; Ding, F.; Lipparini, F.; Egidi, F.; Goings, J.; Peng, B.; Petrone, A.; Henderson, T.; Ranasinghe, D.; Zakrzewski, V. G.; Gao, J.; Rega, N.; Zheng, G.; Liang, W.; Hada, M.; Ehara, M.; Toyota, K.; Fukuda, R.; Hasegawa, J.; Ishida, M.; Nakajima, T.; Honda, Y.; Kitao, O.; Nakai, H.; Vreven, T.; Throssell, K.; Montgomery, J. A., Jr.; Peralta, J. E.; Ogliaro, F.; Bearpark, M. J.; Heyd, J. J.; Brothers, E. N.; Kudin, K. N.; Staroverov, V. N.; Keith, T. A.; Kobayashi, R.; Normand, J.; Raghavachari, K.; Rendell, A. P.; Burant, J. C.; Iyengar, S. S.; Tomasi, J.; Cossi, M.; Millam, J. M.; Klene, M.; Adamo, C.; Cammi, R.; Ochterski, J. W.; Martin, R. L.; Morokuma, K.; Farkas, O.; Foresman, J. B.; Fox, D. J. *Gaussian 16*, Revision A.03; Gaussian, Inc.,: Wallingford, CT, 2016.
(51) Řezáč, J.; Fanfrliék, J.; Salahub, D.; Hobza, P. *J. Chem. Theory Comput.* **2009**, *5*, 1749−1760.
(52) Dennington, R.; Keith, T. A.; Millam, J. M. *Gauss View*, Version 6; Semichem Inc.: Shawnee Mission, KS, 2016.
(53) Jónasdóttir, H. S.; Papan, C.; Fabritz, S.; Balas, L.; Durand, T.; Hardardottir, I.; Freysdottir, J.; Giera, M. *Anal. Chem.* **2015**, *87*, 5036−5040.
(54) Liu, C.; Le Blanc, J. C. Y.; Shields, J.; Janiszewski, J. S.; Ieritano, C.; Ye, G. F.; Hawes, G. F.; Hopkins, W. S.; Campbell, J. L. *Analyst* **2015**, *140*, 6897−6903.
(55) Psutka, J. M.; Dion-Fortier, A.; Dieckmann, T.; Campbell, J. L.; Segura, P. A.; Hopkins, W. S. *Anal. Chem.* **2018**, *90*, 5352−5357.
(56) Wernisch, S.; Afshinnia, F.; Rajendiran, T.; Pennathur, S. *Anal. Bioanal. Chem.* **2018**, *410*, 2865−2877.
(57) Berthias, F.; Maatoug, B.; Glish, G. L.; Fathi Moussa, F.; Maître, P. *J. Am. Soc. Mass Spectrom.* **2018**, *29*, 752−760.
(58) Bowman, A. P.; Abzalimov, R. R.; Shvartsburg, A. A. *J. Am. Soc. Mass Spectrom.* **2017**, *28*, 1552−1561.
(59) Pathak, P.; Baird, M. A.; Shvartsburg, A. A. *Anal. Chem.* **2018**, *90*, 9410−9417.
(60) Ray, J. A.; Kushnir, M. M.; Yost, R. A.; Rockwood, A. L.; Meikle, A. W. *Clin. Chim. Acta* **2015**, *438*, 330−336.
(61) Wei, M. S.; Kemperman, R. H. J.; Yost, R. A. *J. Am. Soc. Mass Spectrom.* **2019**, *30*, 731−742.
(62) Lintonen, T. P. I.; Baker, P. R. S.; Suoniemi, M.; Ubhi, B. K.; Koistinen, K. M.; Duchoslav, E.; Campbell, J. L.; Ekroos, K. *Anal. Chem.* **2014**, *86*, 9662−9669.
(63) Seymour, J. L.; Costello, C. E.; Zaia, J. *J. Am. Soc. Mass Spectrom.* **2006**, *17*, 844−854.
(64) Harvey, D. J.; Rudd, P. M. *Int. J. Mass Spectrom.* **2011**, *305*, 120−130.
(65) Walker, S. W. C.; Anwar, A.; Psutka, J. M.; Crouse, J.; Liu, C.; Le Blanc, J. C. Y.; Montgomery, J.; Goetz, G. H.; Janiszewski, J. S.; Campbell, J. L.; Hopkins, W. S. *Nat. Commun.* **2018**, *9*, 5096.

DOI: 10.1021/acs.analchem.9b01595
Anal. Chem. 2019, 91, 9916−9924